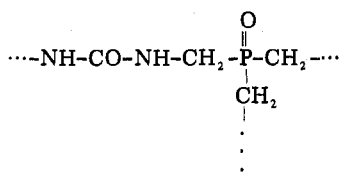In the technical application, the polymer is formed by padding an aqueous solution containing the phosphonium salt and urea onto the fabric which is then heat-cured. The durability of the treatment is enhanced by post-oxidation with hydrogen peroxide to form the more stable phosphine oxide structure; this oxidized polymer may be represented by VII.

$$\cdots\text{-NH-CO-NH-CH}_2\text{-}\overset{\displaystyle\overset{O}{\|}}{\underset{\displaystyle\underset{\vdots}{\overset{|}{\text{CH}_2}}}{\text{P}}}\text{-CH}_2\text{-}\cdots$$

VII

The cross-linked polymer is chemically inert and therefore not capable of interacting with the cellulose fiber. However, it has been shown that at temperatures above 240 °C the polymer is thermally degraded to water-soluble products, among which phosphoric acids and phosphoramidates have been isolated. In the case of the tetrakis(hydroxymethyl)phosphonium salt/urea system, therefore, the effective flame-retardant moieties are not present initially but are generated only in the course of the thermal degradation of the flame-retardant polymer.[35]

Conclusions

Highly effective phosphorus-based flame retardants for a variety of polymeric materials have been developed. As the use of synthetic polymer materials continues to increase while, at the same time, the general public is becoming more aware of the inherent flammability hazards of these materials, the need for even better flame retardants will remain strong. Not only will future flame retardants be required to reduce the hazards of flaming combustion, but at the same time, their effect on the generation of smoke and toxic gases in fire situations will become increasingly important. Similarly, the effects of flame retardants on health and environment is coming under close scrutiny. From what we know today, these additional demands are likely to increase further the importance of phosphorus derivatives vs. systems based on other elements.

(35) U. Einsele, *Melliand Textilber. Int.*, 57 (1), 64 (1976).

Laser-Induced Vibrational Energy Transfer Kinetics: Methyl and Methyl-d_3 Halides

BOYD L. EARL, LEONARD A. GAMSS, and AVIGDOR M. RONN*

Department of Chemistry, Brooklyn College of the City University of New York, Brooklyn, New York 11210

Lasers came to the foreground early in their chemical careers in the study of energy-transfer processes at all levels of excitation. The flow of energy in nonreactive as well as reactive systems has great significance in both fundamental and practical forms. Relaxation processes, those by which an induced nonequilibrium distribution of populations decays back to normal statistical conditions, have been studied by a variety of techniques, including shock tubes, ultrasonic dispersion, excitation with conventional radiation sources, temperature and pressure jump, and, most recently, the use of lasers as tools for creating the initial nonequilibrium situation. These studies may yield a good deal of information concerning intermolecular potentials, but perhaps their greater impact will be in providing a general picture of pathways by which molecular energy flows.

Lasers have singular advantages over most excitation methods in that they make possible excitation of a specific energy level (by their nearly monochromatic nature) and, in addition, induce a significant excess population in that level (by their intensity). Having a system "prepared" in a specific state allows one to extract much more detailed information concerning relaxation rates and pathways than would otherwise be possible.

Let us refer specifically to the situation of molecular vibrational energy transfer. The classical ultrasonic dispersion technique has been used to measure overall relaxation rates for many species. Only recently, and by use of rather complicated deconvolution techniques, has any effort been made to deduce rate constants for specific pathways, e.g., from one excited vibrational level to another within the same species. Laser excitation provides direct access to such information. The procedure, which will be discussed in some detail below, involves direct placement of an excess few percent of the molecules in a sample into a specific vibrational level. Subsequently, one follows the time evolution of fluorescence emission from as many other vibrational levels as possible. Clearly, the access to detailed information concerning the collisional relaxation mechanisms is greatly enhanced.

Avigdor M. Ronn was born in Israel, and is now Professor of Chemistry at Brooklyn College and Chairman of the Physical Chemistry Division of the City University of New York. After completion of his undergraduate studies at the University of California, Berkeley, he went on to graduate study at Harvard University, where he received the Ph.D degree in 1966. He spent 2 years in postdoctoral research at National Bureau of Standards and was on the faculty at Polytechnic Institute of New York before moving to Brooklyn College in 1973. Dr. Ronn's research centers on laser chemistry, isotope separation, particulate formation, and kinetics.

Boyd L. Earl is an Assistant Professor of Chemistry at University of Nevada, Las Vegas. He received his Ph.D. degree from University of California, Berkeley, in 1973. Leonard A. Gamss received his Ph.D. degree from Polytechnic Institute of Brooklyn in 1975, and is now with the Chemistry Department of Bar-Ilan University, Ramat-Gan, Israel.

Knowledge of energy flow pathways takes on its greatest impact when applied to problems involving chemical reactions. One's initial exposure to energy vis-à-vis reaction rates usually comes in the form of the Arrhenius equation, rate constant = $Ae^{-E_a/kt}$, where A is the preexponential factor, k is the Boltzmann constant, T the absolute temperature, and E_a the activation energy, which is obtained experimentally from measurements of rate as a function of T. With the advent of photochemistry researchers began to attack the problem of rate dependence on energy deposited into specific degrees of freedom of the reactants. Recently knowledge in this field has been advanced by molecular beam studies, modern trajectory calculations, and a large number of studies in which laser excitation of specific degrees of freedom was used. Combined studies using both beam and laser techniques provided an extra dimension of finesse. The other side of this question, disposition of product energy, has also been subject to widespread investigation by the foregoing techniques as well as chemical laser and chemiluminescence studies. The two sides of the question are, of course, the two sides of the equal sign in the principle of microscopic reversibility.

The utility of energy-transfer information in this general area of inquiry becomes clear when one asks how energy introduced into a specific vibrational normal mode of a polyatomic molecule affects that molecule's availability for some particular reactive process. Understanding what the excited species itself does with the energy is clearly a prerequisite to any clear mechanistic interpretation of the effects of the excitation on a reaction rate.

While the methyl halides and their fully deuterated counterparts are perhaps not of great interest as reactive species, they are ideal for energy-transfer studies, mainly because they all show absorptions of CO_2-laser lines. In undertaking the investigation of these two series, we hoped to provide two things: (1) a test of available, relatively simple theoretical models, and (2) a predictive capacity, based on these models and/or the wisdom born of the experience of doing these studies. Energy-transfer studies of similar species with specific differences were of particular interest to us. This choice of system came partly because the extractable information lends itself well to theoretical modelling and partly because our predictive capabilities were thus challenged.

While currently acceptable theories in vibration to vibration (V–V), vibration to translation (V–T), or vibration to rotation (V–R) energy transfer are hardly quantitative, we nonetheless show good general qualitative trends within homologous series. Our predictive capacity, when tested against the final species studies, was quite good. In summary, we believe that the results of this work will generally enhance the appreciation of vibrational energy transfer studies in the large number of chemical areas to which such results are applicable.

Experimental Techniques

The experimental system, described in detail elsewhere[1], has as its principal component a Q-switch CO_2–N_2–He laser. A total of 60 odd frequencies ranging

Table I.
Activation Rate Data

	ν_2, ν_5	ν_1, ν_4	ν_3	ν_6
CH_3F	86^a	122		
	106^b	77	f	e
	-315^c	d		
CH_3Cl	160	214	76	
	53	39	110	f
	-330	d	285	
CH_3Br	105	108	40	
	64	62	170	f
	-360	d	340	
CH_3I	101	225		
	65	32	e	f
	-370	d		
CD_3F		680		
	e	12	f	e
		d		
CD_3Cl		490	52	52
	f	17	150	150
		d	260	260
CD_3Br		650	86	86
	f	10	77	77
		d	280	280
CD_3I	f	780	92	92
		10	80	80
		d	295	295

^{a} The first number in each section is the rate constant for the activation process in units of ms^{-1} $Torr^{-1}$. ^{b} The second number in each section represents Z, the number of collisions needed for activation. Parameters used to calculate Z were obtained from ref 16. ^{c} The third number in each section represents the energy deficit (cm^{-1}) between the energy levels involved in the rate-determing step. ^{d} No mechanism proposed. ^{e} Rate constant not measurable due to experimental difficulties (laser scatter, weak signal, fast signal). ^{f} Denotes the laser-pumped level.

between 9.2 and 11.2 μ are available. Typical laser parameters are outputs of 4 mJ per pulse, pulse lengths of 0.5–1.5 μs and repetition rates of 10–400 s^{-1}. The laser beam is passed through a gas sample cell equipped with NaCl windows and is monitored via a monochromator and a high-speed infrared (IR) detector. Fluorescence is observed at right angles to the laser beam axis through a third window on the gas cell. The window material can be chosen as a filter to block the scattered laser light. Interference filters further isolate the signal of interest. Since IR fluorescence is inherently very weak, data are normally gathered over very many laser pulses; 300 000 is not uncommon. Typically a boxcar integrator or a waveform eductor is used for signal processing. From the resulting curve of relative fluorescence intensity vs. time, one obtains rates of rise and/or decay of emission from the level under investigation. A plot of the rate vs. gas pressure can then be made, and the slope of such a plot will yield the rate constant for vibrational energy transfer into or out of the level. Such measurements are made for every observable fluorescing state in the species, and thus a map of the energy flow can be obtained.

Results

The results of experiments and calculations on the normal and deuterated methyl halides are presented in Figures 1 and 2[2-15] and Tables I–III.[16-20] Figures 1 and

(1) G. W. Flynn, in "Chemical and Biochemical Applications of Lasers", C. B. Moore, Ed., Academic Press, New York, N.Y., 1974.

(2) B. L. Earl, P. C. Isolani, and A. M. Ronn, *Chem. Phys. Lett.*, **39**, 95 (1976).

(3) E. Weitz, G. W. Flynn, and A. M. Ronn, *J. Chem. Phys.*, **56**, 6060 (1972).

Table II
Deactivation Rate Data

	Self	He	Ne	Ar	Kr	Xe
CH_3F	0.59^a	0.78	0.065	0.039	0.022	0.019
	15300^b	17300	117000	195000	315000	387000
CH_3Cl	7.5	3.1	0.51	0.54	0.54	0.53
	1100	4800	15000	14000	12000	13000
CH_3Br	20	4.2	1.2	1.3	1.0	1.0
	300	3700	6300	5500	5900	5700
CH_3I	22	5.6	1.9	2.2	1.6	1.3
	500	4000	4600	4400	4800	5600
CD_3F	0.44	1.6	0.12	0.074	0.025	0.082
	18000	8300	65000	102000	222000	86000
CD_3Cl	2.8	7.3	0.48	0.17	0.12	0.13
	2900	2000	17000	44000	55000	52000
CD_3Br	12	7.4	1.2	1.1	1.0	0.70
	600	1800	6400	6500	5700	9300
CD_3I	27	13	1.6	1.7	1.8	1.4
	400	1800	7100	5900	4400	5300

[a] First number is rate constant for V-T/R deactivation process in ms^{-1} $Torr^{-1}$.   [b] Second number is Z, number of collisions needed for deactivation, rounded off to the nearest hundred.

Table III
Normal Mode Data

	CH_3F	CH_3Cl	CH_3Br	CH_3I	CD_3F	CD_3Cl	CD_3Br	CD_3I
$\nu_1{}^a$	2930	2937	2935	2933	2110	2160	2160	2130
$B_1{}^b$	500	235	215	147	310	152	117	82
$\langle A_1{}^2 \rangle^c$	0.24	0.24	0.24	0.24	0.12	0.11	0.12	0.11
ν_2	1464	1355	1306	1252	1136	1029	992	951
B_2	45	91	186	276	70	144	151	184
$\langle A_2{}^2 \rangle$	0.22	0.22	0.22	0.22	0.060	0.09	0.091	0.090
ν_3	1049	732	611	533	991	701	577	501
B_3	1450	310	115	26	900	206	90	13
$\langle A_3{}^2 \rangle$	0.019	0.027	0.030	0.040	0.058	0.033	0.035	0.030
ν_4	3006	3039	3056	3060	2258	2283	2297	2298
B_4	500	130	61	29	250	69	29	9.2
$\langle A_4{}^2 \rangle$	0.23	0.22	0.22	0.22	0.10	0.10	0.098	0.10
ν_5	1466	1452	1443	1436	1072	1060	1056	1049
B_5	80	165	160	142	45	93	95	84
$\langle A_5{}^2 \rangle$	0.23	0.24	0.24	0.24	0.11	0.11	0.10	0.11
ν_6	1182	1017	955	882	903	768	713	656
B_6	23	54	96	119	6	15	27	43
$\langle A_6{}^2 \rangle$	0.22	0.22	0.22	0.22	0.096	0.10	0.12	0.17

[a] Band center frequency of the designated normal mode in cm^{-1}.   [b] Integrated band intensity in units of 10^{10} cps/cm.[17,18]
[c] Breathing sphere parameters in amu^{-1}, calculated using normal mode analysis in ref 19 and 20.

2 show partial vibrational energy level diagrams for these species. The rate constants are given in units of ms^{-1} $Torr^{-1}$, which means that at 1 Torr gas pressure the signal would display an exponential behavior given

by e^{-kt} for a decaying signal or $1 - e^{-kt}$ for a rising signal where k is a rate constant and t is time in ms. Alternatively, one could present the data as Z, the average number of gas-kinetic collisions required to achieve a single energy-transfer event. This number is obtained simply by dividing the gas kinetic collision rate at 1 Torr, $z_g = 2.56 \times 10^6((\sigma_a + \sigma_b)/2)^2 \mu^{-1/2}$, by $10^3 k$, where σ_a, σ_b, and μ are the diameters (Å) and reduced mass (amu), respectively, of the collision partners and k is the rate constant as above. Z has the advantage of reflecting more directly than k the relative efficiency of a process. Tables I and II present the data for activation (fluorescence rise) and deactivation (fluorescence fall), respectively, of all the processes studied, in terms of k and Z. Also presented are the energy defects for the most probable mechanistic pathway, if this pathway is felt to be relatively certain. Table III presents, for each normal mode of each species under consideration, the zero-order energy, in cm^{-1}, the integrated band strength for the corresponding optical transition, indicated by B_i, and finally a number indicated by $\langle A_i{}^2 \rangle$, known as the breathing-sphere parameter, which correlates directly with the amplitude of the motion associated with the ith normal mode. As

(4) Z. Karny, A. M. Ronn, E. Weitz, and G. W. Flynn, *Chem. Phys. Lett.*, **17**, 347 (1972).
(5) E. Weitz and G. W. Flynn, *J. Chem. Phys.*, **58**, 2679 (1973).
(6) E. Weitz and G. W. Flynn, *J. Chem. Phys.*, **58**, 2781 (1973).
(7) J. T. Knudtson and G. W. Flynn, *J. Chem. Phys.*, **58**, 2684 (1973).
(8) S. M. Lee and A. M. Ronn, *Chem. Phys. Lett.*, **22**, 279 (1973).
(9) F. R. Grabiner and G. W. Flynn, *J. Chem. Phys.*, **60**, 398 (1974).
(10) B. L. Earl and A. M. Ronn, *Chem. Phys.*, **12**, 113 (1976).
(11) Y. Langsam, S. M. Lee, and A. M. Ronn, *Chem. Phys.*, **14**, 375 (1976).
(12) L. A. Gamss, B. H. Kohn, and A. M. Ronn, *Chem. Phys. Lett.*, **41**, 413 (1976).
(13) L. A. Gamss, B. H. Kohn, M. I. Pollack, and A. M. Ronn, *Chem. Phys.*, **18**, 85 (1976).
(14) S. T. Lin, B. L. Earl, and A. M. Ronn, *Chem. Phys.*, **16**, 117 (1976).
(15) Y. Langsam, S. M. Lee, and A. M. Ronn, *Chem. Phys.*, **15**, 43 (1976).
(16) J. O. Hirschfelder, C. F. Curtis, and R. B. Bird, "Molecular Theory of Gases and Liquids", Wiley, New York, N.Y., 1954.
(17) G. M. Barrow and D. C. McKean, *Proc. R. Soc. London, Ser. A*, **213**, 27 (1952).
(18) A. D. Dickson, I. M. Mills, and B. Crawford, Jr., *J. Chem. Phys.*, **27**, 45 (1957).
(19) J. Aldous and I. M. Mills, *Spectrochim. Acta*, **18**, 1073 (1962).
(20) W. T. King, I. M. Mills, and B. L. Crawford, Jr., *J. Chem. Phys.*, **27**, 455 (1957).
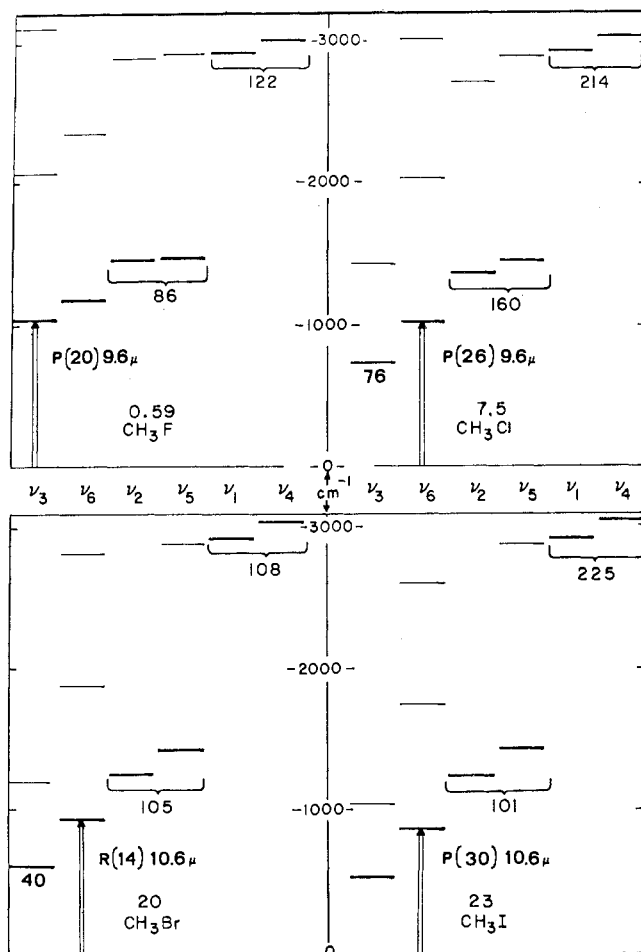
Figure 1. Partial energy level and collisional transfer diagrams for the methyl halides. Heavy lines are fundamentals and lighter lines are overtones. The laser absorption process is shown by an arrow indicating the CO_2 laser pumping line and the initially excited level. The numbers associated with other levels or groups of levels are the rate constants measured for the rise of the fluorescence signal from these levels following laser excitation. The number at the bottom center of each panel is the rate constant for the decay of the fluorescence signals measured from all excited levels. All rate constants are in units of ms^{-1} $Torr^{-1}$. References: CH_3F, 2–6; CH_3Cl, 7–9; CH_3Br, 10; CH_3I, 11. Reproduced with permission from ref 11; copyright 1976 North Holland Publishing Co.

discussed below, the energy defects, the B_i values, and the $\langle A_i^2 \rangle$ values are all important in interpreting the detailed mechanism of energy transfer in these species.

Discussion

As we attempt to develop a systematic understanding of energy transfer in the methyl halides, a few preliminary remarks on collisional transfer in the vibrational regime are in order. Upon laser irradiation, a certain fraction of molecules in our gaseous sample of CH_3X is excited to some state, say ν_i. We may consider two broad classes of energy transfer processes, vibration to vibration (V–V) and vibration to translation–rotation (V–T/R), and further subdivide the former. Initially let us consider collisions of two excited molecules to populate an overtone:

$$CH_3X(\nu_i) + CH_3X(\nu_i) \rightleftarrows CH_3X(2\nu_i) + CH_3X(0) + \Delta E(\text{small}) \tag{1}$$
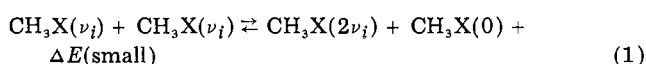
Such "up-the-ladder" processes within a single manifold, being nearly resonant, are expected to be very
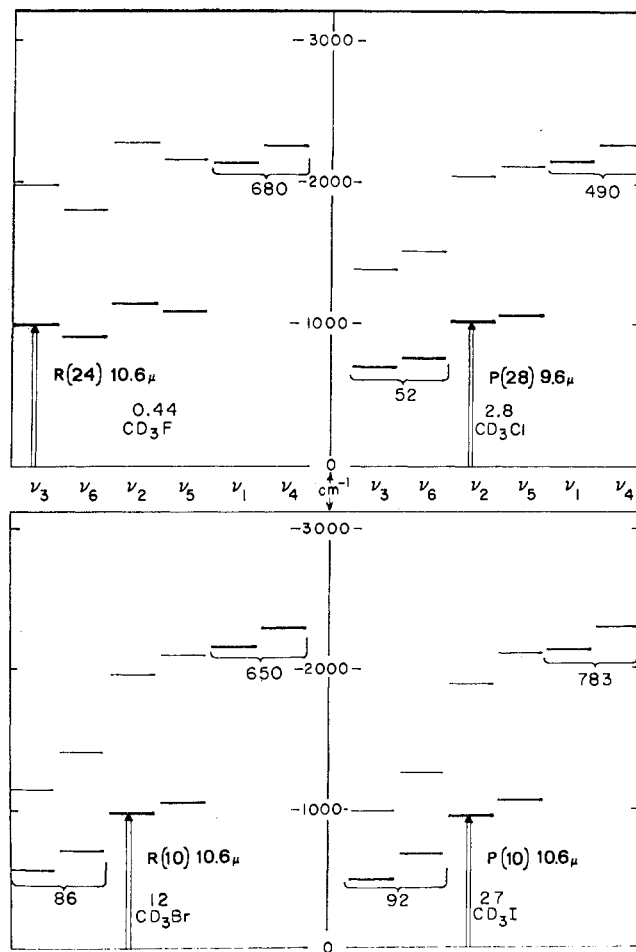
Figure 2. Partial energy level and transfer diagrams for the methyl-d_3 halides. Conventions as in Figure 1. References: CD_3F, 12; CD_3Cl, 13; CD_3Br, 14; CD_3I, 15.

efficient. In the few cases where experimental measurements have been made, cross sections of approximately one-fifth to one-third gas kinetic magnitude have been found.[2] Similar behavior is expected and found in populating combination bands by collisions of molecules in two different excited states.

A second type of V–V process is one in which one member of the colliding pair is initially in the ground state, and the collision produces a molecule in a different excited state:

$$CH_3X(n\nu_i) + CH_3X(0)(\text{or M}) \rightleftarrows CH_3X(m\nu_j) + CH_3X(0)(\text{or M}) + \Delta E \tag{2}$$
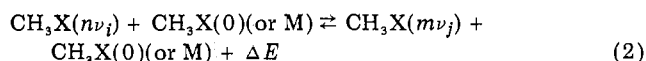
Here the energy defect ΔE is determined by the levels of the states involved, and may be quite large. These processes will be primarily responsible for distributing the excess vibrational energy among all the normal modes following the initial mode-specific excitation. Note that the collision partner may be a molecule of a different species, such as a rare gas atom (M).

In V–T/R transfer, an excited molecule collides with another molecule and loses its excess vibrational energy, which is converted into translational and rotational energy.

$$CH_3X(\nu_i) + CH_3X(\text{or M}) \rightleftarrows CH_3X(0) + CH_3X(\text{or M}) + \Delta E = E_i \tag{3}$$
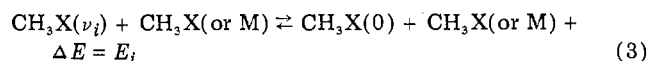
The energy defect in such a process is simply equal to the energy of the level which is deactivated, typically

several hundred wavenumbers. The collision partner in this case may be in any state, and may again be a molecule of a different species.

While processes of this type are normally referred to as V–T/R, it is worth pointing out that any energy transfer process which is not perfectly resonant in the vibrational energies has a V–T/R component. Energy conservation demands that the energy defect in a V–V process be compensated for precisely by changes in the translational and rotational energies. Thus it is at least possible for significant V–T/R decay to occur without any direct V–T/R processes, such as eq 3 above.

The energy defects of the types of processes above have been emphasized because it is this factor, probably more than any other single parameter, which determines the efficiency of a collisional energy-transfer process. A theory of such processes in the hard-collision regime, that dominated by the repulsive part of the intermolecular potential, was developed by Schwartz, Slawsky, and Herzfeld (SSH)[21,22] and later modified by Stretton[23] and Tanczos.[24] In this theory, the probability per gas kinetic collision that an energy-transfer event will occur is proportional to the product of an integral over available collision energies, which brings in the energy defect information, and the breathing sphere parameters $\langle A_i^2 \rangle$, for the normal modes involved. This parameter, which gives the mean Cartesian displacement of the surface atoms of a molecule for a unit change in a particular normal coordinate and thus correlates with the amplitude of the motion in that coordinate, functions as a matrix element in the theoretical probability expression. The breathing sphere parameters are calculable from a normal mode analysis of the molecule. For the CH_3X and CD_3X series, the general pattern of the $\langle A_i^2 \rangle$ values, which are given in Table III, is very similar. For all modes except ν_3, the values are approximately equal throughout a series, while the $\langle A_3^2 \rangle$ values are smaller and vary from one member of the series to another. This is expected, since ν_3 involves the C–X stretching motion, which changes with the halogen substituent, while the remaining modes involve motions of H or D atoms, which do not change within a series. In addition, since these latter modes involve motions of lighter atoms, they have larger amplitudes, which are reflected in their larger $\langle A_i^2 \rangle$ values. Note also that the $\langle A_i^2 \rangle$ values for the H-dominated modes are all approximately twice as large as those for the D-controlled motions. There appears to be an anomaly in the pattern at $\langle A_2^2 \rangle$ and $\langle A_3^2 \rangle$ of CD_3F, which is traceable to a large coupling term of the corresponding symmetry coordinates in the normal mode analysis.

We wish now to explore any apparent relationships between energy defects and breathing-sphere parameters on the one hand and experimentally observed energy-transfer efficiencies on the other. As implied above, we anticipate a positive correlation between efficiency and the breathing sphere parameters and a strong negative correlation between efficiency and energy defects. The specification of energy defects depends on the assignment of a mechanism for the

process in question. (Frequent reference to Figures 1 and 2 will help clarify the following discussion.) As one example, in the case of the ν_3 activation in CH_3Cl, the only reasonable mechanism would seem to be a direct collisional transfer from the pumped state:

$$CH_3Cl(\nu_6) + CH_3Cl(0) \rightleftarrows CH_3Cl(\nu_3) + CH_3Cl(0) + \Delta E = 280 \text{ cm}^{-1} \quad (4)$$
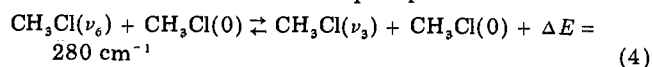
Activation of the ν_1,ν_4 levels in the CH_3X series presents a different case. There are at least two mechanisms which appear equally attractive, each involving several energy-transfer steps. One is up-the-ladder activation of the $3\nu_p$ state, where ν_p is the pumped state, followed by an intermode crossover step from $3\nu_p$ to ν_1,ν_4; the other is initial transfer from ν_p to ν_2,ν_5, hence to $2\nu_2,2\nu_5$, and across to ν_1,ν_4 (this route is perhaps somewhat favored because of Fermi resonance between $2\nu_5$ and ν_1). The interdeterminacy in the mechanism, as well as the several steps involved, each with its attendance energy defects and breathing sphere parameters, leads us to omit these processes from any attempt at quantitative comparisons. An intermediate case in terms of each assignment is the activation of ν_2,ν_5 in the CH_3X series. One is tempted to assign a direct transfer from ν_p to ν_2,ν_5 as the mechanism, and for purposes of our comparison we have tentatively done so. We have also assumed that activation proceeds directly by transfer from ν_p to the ν_2 state, and then to ν_5 by a step with a small energy defect.

We can, however, propose a different mechanism for ν_2,ν_5 activation. If ν_1,ν_4 are activated via $3\nu_p$, as discussed above, then a crossover may occur from $\nu_1\nu_4$ over to $2\nu_2,2\nu_5$, and down to ν_2,ν_5. This "around the horn" mechanism cannot be ruled out, but again is too complicated to provide any satisfying information in a simple correlation.

One is faced with a similar, though ultimately less difficult, problem in looking at the activation of the low-lying levels (ν_3 and ν_6) in CD_3Cl, CD_3Br, and CD_3I. In all three cases, there is at first a choice to be made between direct transfer down to these levels from the pumped state and a transfer mechanism which would proceed via the overtones, $2\nu_3$ and $2\nu_6$, which would involve smaller energy defects in some cases. We tend to discount the latter because of the generally smaller (by at least an order of magnitude) contributions of overtones as opposed to fundamentals. However, we must note that in the CD_3I case there is a very near resonance between ν_2 and $2\nu_3$, which should enhance the probability of this route. Further questions in these three species are: which level is the recipient of the transfer (is the activation a series $\nu_2 \rightarrow \nu_6 \rightarrow \nu_3$ or a parallel $\nu_2 \rightarrow \nu_6$, $\nu_2 \rightarrow \nu_3$ route) and which level is observed in the fluorescence signal? In CD_3Br and CD_3I, both levels fall within the transmission curves of the filters which were used. From Table III we see that in CD_3Br the ν_3 mode has a larger B value than does ν_6, whereas in CD_3I the opposite is true. In both cases, we should expect the fluorescence to be composed mainly of emission from the level with the larger B value, but the differences in these values are such that the other level should contribute significantly. We assume that ν_3 is activated by a series mechanism, as direct $\nu_2 \rightarrow \nu_3$ transfer involves an energy defect of more than 400 cm^{-1} in both cases, while a $\nu_6 \rightarrow \nu_3$ step requires conversion of only about 140 cm^{-1}. CD_3Cl presents a special case

(21) R. N. Schwartz, Z. I. Slawsky, and K. F. Herzfeld, *J. Chem. Phys.,* **20**, 1591 (1952).

(22) R. N. Schwartz and K. F. Herzfeld, *J. Chem. Phys.,* **22**, 767 (1954).

(23) J. L. Stretton, *Trans. Faraday Soc.,* **61**, 1053 (1965).

(24) F. R. Tanczos, *J. Chem. Phys.,* **25**, 439 (1965).

as ν_3 fluorescence was isolated and the activation rate constant of 52 ms^{-1} Torr^{-1} was measured for this level alone. However, observation of both levels did not yield a significantly different result, so we may assume that this rate constant reflects the behavior of both levels (note that B for ν_6 is 14 times smaller than that for ν_3, so the fluorescence signal in the combined measurement was almost completely due to the lower level). It is not so clear in this case that a series mechanism is preferred over a parallel one for the filling of ν_3 and ν_6. This is mainly because these levels lie much nearer each other in CD$_3$Cl than in the two species which follow it in the series. We have assumed a series mechanism for purposes of this comparison, but let it be noted that a direct $\nu_2 \rightarrow \nu_6$, $\nu_2 \rightarrow \nu_3$ transfer would fit the correlation pattern much better.

This, along with the results of the correlation, can be seen in Table I. For the ν_2,ν_5 activation in the CH$_3$X series, where all the $\nu_p \rightarrow \nu_2$ energy defects are quite similar, the requisite number of collisions agrees quite closely for the lowest three numbers, which involve $\langle A_i^2 \rangle$ values of 0.22 for the states on both ends of the transfer process. For CH$_3$F, where approximately twice as many collisions are required even though the ΔE value is the lowest in the series, we note that the participation of ν_3, which is the pumped state, introduces a smaller breathing sphere parameter. The activation of the low-lying levels presents some interesting comparisons. In CH$_3$Cl and CH$_3$Br, we are looking at analogous processes with essentially equal $\langle A_i^2 \rangle$ values for both states, and the effect of the larger ΔE value in CH$_3$Br seems apparent. Comparing CH$_3$Cl and CD$_3$Br, with nearly equal energy defects, the larger $\langle A_i^2 \rangle$ product for the latter species may explain the greater efficiency of the process there. CD$_3$I is quite comparable to CD$_3$Br in the values involved in this comparison. CD$_3$Cl appears to be the only member of our group which does not fit well in this, and, as mentioned, the ΔE and $\langle A_i^2 \rangle$ value here assume a series mechanism for activation of ν_3, so we actually use parameters appropriate to ν_6 in the comparison. If we assume a direct $\nu_2 \rightarrow \nu_3$ activation and use the appropriate parameters, we see that a ΔE of 330 cm^{-1} and $\langle A_i^2 \rangle$ values of 0.09 and 0.033 fit into the correlation scheme very nicely.

There are obviously imperfections in this scheme, and one could not expect to obtain quantitatively accurate predictions, but, especially in situations where one is considering analogous processes, the direction of the change in the efficiency seems to correlate reasonably well with what one would expect from simple considerations of energy defects and breathing sphere parameters.

The activation of the ν_1,ν_4 states in the CD$_3$X series has not yet been discussed. These processes stand apart from the others measured by virtue of their extreme rapidity. The rate constants all approach the values found for nearly resonant up-the-ladder type processes, and this is not really surprising when one considers that the proximity and overlapping character of the ν_2 and ν_5 states, coupled with the Fermi resonance between $2\nu_5$ and ν_1, provides a very direct path by which energy injected into ν_2 can reach ν_1. The $2\nu_5$ state itself has a significant B value, and the fluorescence from the Fermi-coupled pair will dominate that from ν_4. In fact,

attempts to observe isolated ν_4 fluorescence with the appropriate filter were made on all the species in the CD$_3$X series and in no case was any signal observed, while the overall signal in the 4–5-μ region was quite strong.

The most striking feature of the results on the V–T/R deactivation of these species is the increase in deactivation efficiency of nearly two orders of magnitude as one proceeds from the fluoride to the iodide in each series. This behavior correlates clearly with the progressive lowering of the energy levels, particularly the two lowest levels ν_3 and ν_6, and illustrates the influence of the energy defect on the efficiency of energy-transfer processes.

If one considers a model system of several levels in which V–V transfer is considerably faster than V–T/R deactivation, which applies quite generally in these species, one can obtain approximate solutions to the kinetic equations which say that the total deactivation rate constant is a weighted sum of the deactivation rate constants from each individual level, with the weighting factor for a level being simply the probability of finding a molecule in that level at the translational temperature of the sample. Strictly speaking, each excited level should contribute to the deactivation. However, due to the effect of the energy defect, only the lowest level or two is expected to contribute significantly. The individual rate constants for the higher levels are much smaller, and, in addition, the Boltzmann weighting factors fall off considerably at higher energies. Calculations based on SSH type V–T theory bear this out; although they do not produce quantitative agreement with experiment, they do indicate significant V–T contributions only from ν_3 and ν_6 in each case. There are two factors which tend to enhance the contribution of ν_6, despite its somewhat higher energy (except in CD$_3$F). These are its double degeneracy and its larger breathing-sphere parameter.

Thus our picture of deactivation in these species is that it proceeds directly from ν_3 or ν_6, while the other levels are deactivated indirectly, as the excess energy funnels into the lowest levels by V–V processes which, by virtue of their speed, maintain a quasi-equilibrium among all the excited levels on the time scale of the deactivation.

A second interesting effect in the deactivation appears in the results on the rare gases which are presented in Figures 3 and 4 as experimental probability per gas kinetic collision vs. the square root of the reduced mass of the collision partners. Pure V–T deactivation, according to SSH type theory, should yield a straight line of negative slope, the slope being steeper for larger energy defects. It is clear that only in the cases of the two fluorides is this behavior approached. For the remaining members of each series, a marked leveling off occurs in these plots. This is quite probably due to the contribution of V–R relaxation to the total probability of deactivation. According to Moore's V–R theory,[25] pure V–R relaxation should yield an essentially horizontal line for each methyl halide because the V–R probability is not a function of the translational velocity and the reduced mass. This in fact is very nearly what is observed for the heavier rare gases with the chlorides, bromides, and iodides. A rough estimate of the relative

(25) C. B. Moore, *J. Chem. Phys.*, **43**, 2979 (1965).
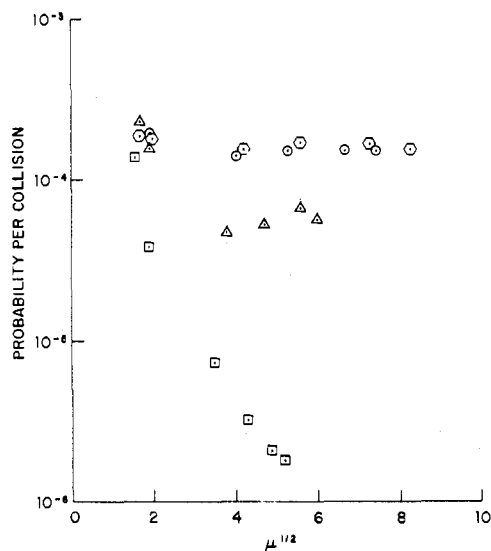
Figure 3. Plot of experimental probability of the rare gas deactivation $(1/Z)$ of the methyl halides vs. the square root of the reduced mass of the collision partners $(amu^{1/2})$. CH_3F-X (squares); CH_3Cl-X (triangles); CH_3Br-X (circles); CH_3I-X (hexagons). See Table II. In cases where six points appear, ^3He was also studied as a deactivator.
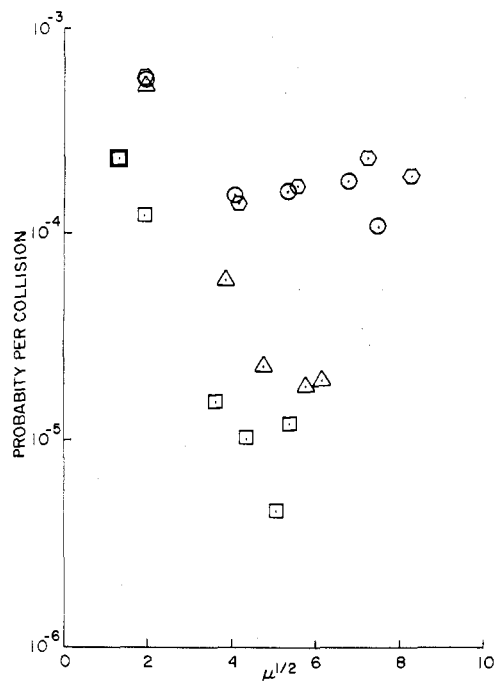
Figure 4. Plot of experimental probability of the rare gas deactivation $(1/Z)$ of the methyl-d_3 halides vs. the square root of the reduced mass of the collision partners $(amu^{1/2})$. CD_3F-X (squares); CD_3Cl-X (triangles); CD_3Br-X (circles); CD_3I-X (hexagons). See Table II. In cases where six points appear, ^3He was also studied as a deactivator.

efficiency of V–R and V–T can be obtained by taking the ratio of the rotational velocity of the methyl halide to the relative translational velocity of the collision partners. If this ratio is significantly greater than unity, V–R is expected to be important. While it is difficult to find a precise crossover point, it is clear that for the heavier collision partners the translational velocity is smaller, while the rotational velocity is nearly constant within each series, since it depends on the moment of inertia of the methyl halide about its symmetry axis. Thus V–R relaxation is expected to become more

important for the heavier rare gases with a given species, and for the heavier methyl halides, as compared to their lighter counterparts. Helium is nearly exempt from this effect, since its own high speed essentially determines the collision speed independently of the partner.

As a final point of comparison, let us consider the V–T/R behavior in a pairwise fashion for each halide species. In each case, the deuterated species possesses lower energy levels than the corresponding normal methyl halide, yet, with the exception of the iodides, the V–T/R decay is less efficient for the CD_3X series. This may appear to contravene earlier assertions concerning the significance of the energy defect, but note first that in these pairs the lowering of the lowest level in particular is relatively slight in each pair. Given this, it would seem that the slower decays in the deuterated species are directly related to the slower, less extensive motions of the deuterium atoms as compared to the hydrogens. This shows up in the smaller breathing-sphere parameters, as discussed, which should make for less efficient V–T decay, while the smaller rotational velocity of the CD_3X series should decrease the efficiency of V–R relaxations as well.

In comparing CH_3X-CD_3X pairs, one notes clear similarity of behavior between the fluorides (if the CD_3F-Xe point may be regarded as an artifact). For the heavier halide pairs the leveling off occurs later for the deuterated partner. This seems particularly evident in the chloride case, where the CH_3Cl–rare gas data begin to level off at Ne while the CD_3Cl–rare gas values decrease further and level off at Ar. This may be stretching the point, but the kinematic effect of deuteration on rotational speed will be much more pronounced than on translational speed, which does correlate well with this trend.

Conclusion

A pattern of V–V and V–T/R energy flow rates has been established in this investigation. Within these series the trend of deactivation times decreasing as the lowest energy levels in the series decrease has been observed. The achievement of vibrational equilibration at a new vibrational temperature prior to V–T/R decay has also been firmly established. The applicability of the SSH theory toward qualitative behavior of both activation and deactivation of molecular states has been tested and found quite satisfactory, and as such our predictive capabilities were tested and found quite effective.

A number of investigators have pointed out that intelligently unravelling laser-driven chemistry will require detailed understanding of the kinetics of each species relaxing from a nonequilibrium distribution resulting from an absorbed laser pulse.

As we have tried to summarize here, the general features of energy-transfer studies point out that mode-selective chemistry is indeed a realizable goal. A number of attempts at laser catalysis of chemical reactions based on information obtained from energy transfer have been reported recently. In all cases when a diatomic molecule was reacted with an atom, enhanced reactivity was observed when the diatomic was laser excited to $V = 1$ or higher vibrational states, consistent with energy-transfer measurements and simple bimolecular kinetics.[26] Where polyatomic

molecules are the reactants, careful evaluation of the relaxation kinetics of the reactants must precede any interpretation of the total mechanism. For example, in the case of CH_3F and Cl_2 reaction,[27] the CH_3F was excited to its C–F stretching mode and the reaction products were found to be CH_2FCl and HCl. Questions regarding intramolecular V–V transfer and intermolecular V–V transfer into the C–H manifold under multiphoton absorption conditions must still be settled before a final mechanism can be deduced.

The value of the energy-transfer information is perhaps best exemplified in recent experiments involving laser isotope separation.[28] If one envisages a reaction driven by laser excitation, a number of immediate constraints on the possible selectivity come to mind. The V–T/R deactivation time of the excited reactant must be longer than the total reaction time. Just as obviously the V–V isotope scrambling rate must be slower than the reaction rate. Therefore, it seems to us that a total understanding, as well as a large data base, of vibrational energy transfer rates in polyatomic species is of import to understanding collisional phenomena in general and to the new and exciting field of laser-induced chemistry. We expect that most polyatomic species will follow the general pattern of energy transfer observed here. Numerous studies on the other systems tend to bear out this expectation. While these may not bear quantitative comparisons with results reported here, we do believe that insights concerning parameters which are significant in vibrational relaxation will retain considerable validity over a very wide range of systems.

(26) Z. Karny, B. Katz, and A. Szoke, *Chem. Phys. Lett.*, **35**, 100 (1975).
(27) B. L. Earl and A. M. Ronn, *Chem. Phys. Lett.*, **41**, 29 (1976).
(28) C. P. Robinson, *Ann. N.Y. Acad. Sci.*, **267**, 81 (1976).

Transition-State Activity Coefficients—A New Mechanistic Tool in the Investigation of Acid-Catalyzed Reactions

Keith Yates* and Tomasz A. Modro*

Department of Chemistry, University of Toronto, Toronto, Ontario, Canada M5S 1A1

Received August 16, 1977

The interpretation of the variation in the rates of acid-catalyzed reactions with changing acidity has presented a considerable challenge to physical organic chemists, particularly as a guide to the complete understanding of the detailed mechanism of such reactions. Various general kinetic treatments have been proposed for investigating the kinetics and mechanisms of such organic reactions in nondilute (i.e., nonideal) acid solutions. Since the kinetic-acidity dependence of acid-catalyzed reactions in dilute to concentrated acid region can be quite variable and complex, even for apparently simple reactions, these general treatments have not been uniformly successful in providing reliable mechanistic criteria. The four main approaches which have been used are the Zucker–Hammett method,[1] the Bunnett hydration parameter treatment,[2] the Yates modification or *r*-parameter treatment,[3] and the Bunnett–Olsen approach.[4]

Keith Yates was born in England and emigrated to Canada in 1948. He was educated at the University of British Columbia where he received a B.A., M.Sc., and Ph.D., and at Oxford University where he took the D.Phil. degree. In 1961 he joined the Department of Chemistry at the University of Toronto, where he is now Professor and Chairman. His main research interests are in physical and theoretical organic chemistry.

Tomasz A. Modro was born and educated in Poland, receiving the Ph.D. degree in 1962 and the degree of Habilitated Doctor in 1969. Postdoctoral work at the University College, London, was followed by an academic appointment at the University of Gdansk. In 1973 he joined the University of Toronto where he is now Assistant Professor of Chemistry. His research is concentrated in structure–reactivity dependence in organophosphorus compounds, aromatic reactivity, and catalysis in strongly acidic media.

Each of these approaches suffers from similar disadvantages and difficulties. The disadvantages are that each method requires (different) assumptions leading to the cancellation of important activity coefficient terms. Each is heavily dependent on the use of Hammett-type acidity functions, with their attendant uncertainties. Each method also depends heavily on the existence of linear log–log relationships, involving some function of the rate constant, the acidity, and possibly the water activity of the reaction medium. The difficulty here is twofold. One is that linear log–log plots are almost legion in physical-organic chemistry, since they are frequently easy to obtain, and it is often difficult to evaluate the statistical significance of such relationships. The second is that, having obtained these linear relationships, the mechanistic interpretation of the slope values (e.g., unity, ω, w, r, or ϕ) is also fraught with difficulty.

A simpler treatment has been proposed which is based on transition-state theory; it uses hydronium ion activities directly. This approach does not involve any assumptions concerning the acidity function behavior of a particular substrate, nor does it involve the water activity of the medium, since it is not a hydration parameter treatment. No cancellations of important

(1) L. Zucker and L. P. Hammett, *J. Am. Chem. Soc.*, **61**, 2791 (1939).
(2) J. F. Bunnett, *J. Am. Chem. Soc.*, **83**, 4978 (1961).
(3) K. Yates and R. A. McClelland, *J. Am. Chem. Soc.*, **89**, 2686 (1967).
(4) J. F. Bunnett and F. P. Olsen, *Can. J. Chem.*, **44**, 1899, 1917 (1966).